Face Recognition in the Thermal Infrared Spectrum

Pradeep Buddharaju, Ioannis Pavlidis*, and Ioannis Kakadiaris

Computer Science Department
University of Houston
Houston, Texas 77204-3010
{braju,pavlidis}@cs.uh.edu ioannisk@uh.edu

Abstract

We present a two-stage face recognition method based on infrared imaging and statistical modeling. In the first stage we reduce the search space by finding highly likely candidates before arriving at a singular conclusion during the second stage. Previous work has shown that Bessel forms model accurately the marginal densities of filtered components and can be used to find likely matches but not a unique solution [1]. We present an enhancement to this approach by applying Bessel modeling on the facial region only rather than the entire image and by pipelining a classification algorithm to produce a unique solution. The detailed steps of our method are as follows: First, the faces are separated from the background using adaptive fuzzy connectedness segmentation. Second, Gabor filtering is used as a spectral analysis tool. Third, the derivative filtered images are modeled using two-parameter Bessel forms. Fourth, high probability subjects are short-listed by applying the L^2-norm on the Bessel models. Finally, the resulting set of highly likely matches is fed to a Bayesian classifier to find the exact match. We show experimentally that segmentation of the facial regions results in better hypothesis pruning and classification performance. We also present comparative experimental results with an eigenface approach to highlight the potential of our method.

1. Introduction

Face recognition is gaining acceptance as a superior biometric method in access control and surveillance. It is touchless, highly automated, and most natural since it coincides with the mode of recognition that we as humans employ on our everyday affairs. Most of the research efforts in this area have focused on visible spectrum imaging [2]. Despite progress, certain problems still remain. Some of them are due to the very nature of the legacy approaches. Images in the visible band are formed primarily due to reflection. Therefore, they depend on the existence of an external light source, which sometimes may be absent (e.g., nighttime). Imagery formed primarily due to reflection is also difficult to process because of the strong dependence on incident angle and light variation.

Recently, there has been an increased interest in face recognition in the thermal infrared spectrum [3, 4]. In this spectral region images are formed primarily due to emission. Therefore, they do not depend on the existence and intensity of an external light source [5, 6]. They are also less dependent on the incident angle of radiation. Several efforts have been made to compare the performance of face recognition methodologies using visible and thermal infrared images [7, 8, 9]. This research highlighted several advantages of performing face recognition in the thermal infrared along with some weaknesses.

In terms of algorithmic approaches, both appearance and geometry-based methods have been applied in the visible and thermal infrared cases. Appearance-based methods like principal component, independent component, and linear discriminant analysis [10, 11, 12, 13, 14] treat the image simply as a matrix of numbers and impose the decision boundary without extracting any geometric features. Even though such approaches are computationally efficient, they do not perform well in challenging conditions such as variable poses and facial expressions. Geometry-based techniques and template matching approaches extract certain features from the face and then impose probability models (or decision boundaries) on these features [15, 16, 17]. Geometric approaches are usually more robust than appearance-based approaches but at an additional computational cost.

Srivastava *et al.* [1, 18] introduced an interesting approach that decomposes the image into spectral rather than geometric features. Their method prunes the hypothesis space by modeling the extracted spectral features through Bessel parametric forms. The algorithm is elegant and computationally efficient. However, the Bessel model is applied to the entire image while only part of it contains facial information. The approach also does not yield a unique solution

*To whom all correspondence should be addressed.

Proceedings of the 2004 IEEE Computer Society Conference on Computer Vision and Pattern Recognition Workshops (CVPRW'04)
1063-6919/04 $ 20.00 IEEE

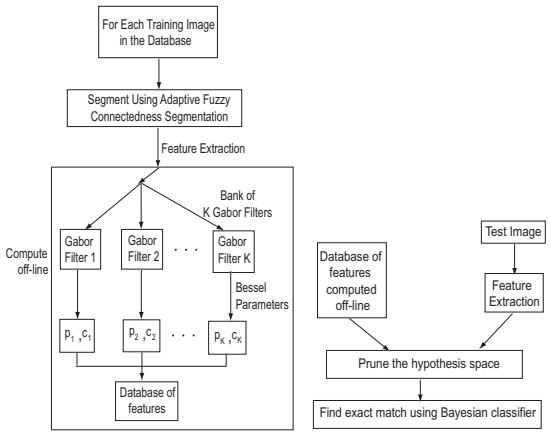

Figure 1: Block diagram of our face recognition method. (a) Training phase. (b)Testing phase.

but rather a set of highly likely solutions.

In this paper, we propose a method that enhances and complements Srivastava's approach. We segment the facial part of the image using adaptive fuzzy connectedness segmentation [19]. Then, we apply Srivastava's algorithm on the facial segment only, not the entire image. This application yields a pruned hypothesis space but not a unique solution. Our method takes a step further and applies Bayesian classification [20] on the pruned hypothesis space to find the exact match. Therefore, our contributions include the introduction and automation of adaptive fuzzy connectedness segmentation and the formation of an end to end classifier (hypothesis pruning plus Bayesian classification). We should emphasize that traditional adaptive fuzzy connectedness is not fully automated as it requires manual selection of a seed pixel.

In Section 2 of this paper we describe our methodology in some detail. In Section 3 we present comparative experimental results and attempt a critical evaluation. We conclude our paper in Section 4.

2. Methodology

Facial images are normally acquired under natural conditions and it is common for such images to contain background. If the entire image is used to obtain features, it may affect the performance of the face recognition system. Hence, we segment the image to remove the background and then decompose the facial segment into its spectral components using a bank of K Gabor filters. Bessel probabilistic models are then imposed on these spectral components to obtain $2K$ Bessel parameters that are used to form the feature vector (see Figure 1(a)).

The Bessel parameters of the database images can be computed off-line and stored for future use as depicted in Figure 1(a). This reduces considerably the on-line computation cost of the algorithm. If a face image is given for testing, the algorithm needs to compute the Bessel parameters of the test image only, prune the hypothesis space, and find the exact match as depicted in Figure 1(b).

2.1. Segmentation

Adaptive fuzzy connectedness segmentation has been successfully applied to segment MRI medical images [19]. We apply a similar approach to segment infrared facial images by providing facial skin pixels as seeds. Fuzzy affinity is assigned to other pixels with respect to these seed pixels.

The fuzzy affinity between two pixels c, d is introduced in [21] as:

$$\begin{aligned} \mu_\kappa(c,d) &= \mu_\alpha(c,d)[\omega_1 h_1(f(c),f(d)) + \omega_2 h_2(f(c),f(d))], \\ \mu_\kappa(c,c) &= 1 \end{aligned} \quad (1)$$

where $\mu_\kappa(c,d)$ is a linear combination of $h_1(f(c),f(d))$ and $h_2(f(c),f(d))$, with $\omega_1 + \omega_2 = 1$. The three features taken into consideration are: the adjacency between the pixels $\mu_\kappa(c,d)$, the intensity of the pixels $h_1(f(c),f(d))$, and the gradient of the pixels $h_2(f(c),f(d))$. The adjacency function $\mu_\alpha(c,d)$ is assumed to be a hard adjacency relation, such as:

$$\mu_\alpha(c,d) = \begin{cases} 1 & \text{iff } \sqrt{\sum_i (c_i - d_i)^2} \leq 1 \\ 0 & otherwise\ , \end{cases} \quad (2)$$

where $c_i,\ d_i,\ (0 \leq i \leq n)$ are the pixels' coordinates in n dimensions. The functions h_1 and h_2 are Gaussian functions of $\frac{1}{2}(f(c)+f(d))$ and $|f(c)-f(d)|$, respectively, such as:

$$\begin{aligned} h_1(f(c),f(d)) &= e^{-\frac{1}{2}[\frac{\frac{1}{2}(f(c)+f(d))-m_1}{s_1}]^2} \\ h_2(f(c),f(d)) &= e^{-\frac{1}{2}[\frac{(|f(c)-f(d)|)-m_2}{s_2}]^2} \end{aligned} \quad (3)$$

where m_1 and s_1 are the mean and standard deviation of the intensities of the sample region and m_2 and s_2 are the mean and standard deviation of the gradient of the sample region. In conventional fuzzy connectedness segmentation [22, 21], ω_1 and ω_2 are free parameters provided by the user and the performance of the algorithm is highly sensitive to the selection of these weight values. In Pednekar *et al.* [19], a method has been developed to compute the weights as adaptive parameters depending on the ratio of homogeneity and gradient function values at each pixel location:

$$\omega_1 = \frac{h_1}{(h_1 + h_2)} \ \ and \ \ \omega_2 = 1 - \omega_1. \quad (4)$$

These adaptive weights minimize user interaction and increase the robustness of the segmentation process.

(a) (b)

Figure 2: (a) Infrared facial image and intermediate multi-seed segmentation results. The selected seeds are represented with white cross marks. (b) Final result of adaptive fuzzy connectedness segmentation.

Pednekar's algorithm assumes that the object to be segmented is relatively homogenized and requires the selection of a single seed. Facial segments in infrared images, however, are typically multi-modal distributions. They feature 'hot' and 'cold' regions. Examples of 'hot' regions include the area around the eyes and forehead. Examples of 'cold' regions include the nose and ears. We have expanded Pednekar's algorithm to select multiple seeds on the basis of sharp gradient changes on facial skin. Then, the algorithm checks for connectedness of other pixels to the respective seeds using the affinity functions (1). The resulting segmented parts are merged to obtain a complete segmented facial image as depicted in Figure 2.

2.2. Feature Extraction

We extract features from segmented images, which can be used for pruning the hypothesis space. As described in Figure 1, this process involves dividing the segmented image into its spectral components using Gabor filters and then modeling these components using Bessel functionals [1, 18]. The Bessel functionals are completely characterized by the Bessel parameters, which form the feature vectors. The L^2-norm is applied to these feature vectors to short-list the best matches.

If $\mathbf{I}$ represents the infrared image and $\mathbf{G}^{(j)}, j = 1, 2, \ldots, K$ represent a bank of K Gabor filters, then $\mathbf{I}^{(j)} = \mathbf{I} * \mathbf{G}^{(j)}, j = 1, 2, \ldots, K$ represent K spectral components of the image $\mathbf{I}$, where $*$ denotes the convolution operation. A number of authors used a bank of Gabor filters to extract local image features[23, 24]. We use the following family of Gabor filters:

$$\mathbf{G}_{\lambda,\sigma,\varphi}(x,y) = e^{-[(x'^2+\gamma^2 y'^2)/2\sigma^2]} \cos\left(2\pi\frac{x'}{\lambda} + \varphi\right) \quad (5)$$

where

$$x' = x\cos\theta + y\sin\theta, \;\; y' = -x\sin\theta + y\cos\theta,$$

$\gamma = 0.5$, $\sigma = 0.56\lambda$, and λ being the spectral number.

For simplicity, we assume in our experiments that the phase angle $\varphi = 0$. Hence, based on different scale (σ) and orientation (θ) values, we obtain a bank of different Gabor filters. Then, we convolve the segmented facial image with each filter in the filter bank to obtain the respective filtered images.

The filtered image $\mathbf{I}^{(j)}$ can be modeled with the following Bessel functional:

$$f(\mathbf{I}^{(j)}(x,y); p, c) = \frac{1}{Z(p,c)} \mid \mathbf{I}^{(j)}(x,y) \mid^{p-0.5} K_{(p-0.5)}\left(\sqrt{\frac{2}{c}} \mid \mathbf{I}^{(j)}(x,y) \mid\right),$$

where Z is a normalizing constant given by:

$$Z(p,c) = \sqrt{\pi}\Gamma(p)(2c)^{0.5p+0.25},$$

and $K_v(x)$ is a modified Bessel function of the second kind expressed in terms of a modified Bessel function of the first kind $I_v(x)$ as:

$$K_v(x) = \left(\frac{\pi}{2}\right)\frac{I_{-v}(x) - I_v(x)}{\sin(v\pi)},$$

$$I_v(x) = \left(\frac{x}{2}\right)^v \sum_{k=0}^{\infty} \frac{\left(\frac{x^2}{4}\right)^k}{k!\,\Gamma(v+x+1)}, \text{ and}$$

$$\Gamma(x) = \int_0^\infty e^{-t}t^{x-1}dt \quad \text{is the gamma function.}$$

The elements of $D = \{f(\mathbf{I}^{(j)}(x,y); p, c) \mid p > 0, c > 0\}$ are referred to as the Bessel forms and the parameters $(\hat{p}^{(j)}, \hat{c}^{(j)}), j = 1, 2, \ldots, K$ as the Bessel parameters. The shape $\hat{p}^{(j)}$ and scale $\hat{c}^{(j)}$ parameters of filtered image $\mathbf{I}^{(j)}$ can be estimated by:

$$\hat{p}^{(j)} = \frac{3}{SK(\mathbf{I}^{(j)})}, \qquad \hat{c}^{(j)} = \frac{SV(\mathbf{I}^{(j)})}{\hat{p}^{(j)}},$$

where SV is the sample variance and SK is the sample kurtosis of the filtered image $\mathbf{I}^{(j)}$ given by:

$$SV = \mu_2, \;\; SK = \frac{\mu_4}{\mu_2^2},$$

where $\mu_k = \frac{\sum_{i=1}^{n}(x_i - \mu)^k}{n}$ (μ is the mean of the filtered image). Figure 3 depicts a segmented infrared facial image and one of its Gabor filtered components.

There is an advantage of representing the segmented infrared images via Bessel forms of their spectral components. The IR images can be compared by directly comparing their corresponding Bessel forms. For this, we define

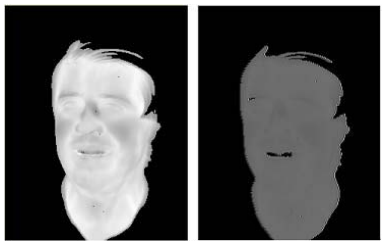

(a) (b)

Figure 3: (a) Segmented infrared facial image. (b) Corresponding Gabor filtered image at scale $\sigma = 2$ and orientation $\theta = 30$, whose Bessel parameters are $p = 0.5617$ and $c = 6694.202$.

the image L^2-norm in the following sense. First, we define the parametric L^2-norm $d(p_1, c_1, p_2, c_2)$ between two Bessel forms $f(\mathbf{I}^{(j)}(x, y); p_1, c_1)$ and $f(\mathbf{I}^{(j)}(x, y); p_2, c_2)$ as [1, 18]:

$$d(p_1, c_1, p_2, c_2) = \sqrt{\left(\frac{\Gamma(0.5)}{2\sqrt{2\pi}}\left(\frac{\mathcal{G}(2p_1)}{\sqrt{c_1}} + \frac{\mathcal{G}(2p_2)}{\sqrt{c_2}} - \frac{2\mathcal{G}(p_1+p_2)}{\sqrt{c_1}}(\frac{c_1}{c_2})^{p_2}\mathcal{F}'\right)\right)},$$

where $\mathcal{G}(p) = \frac{\Gamma(p-0.5)}{\Gamma(p)}$, $\mathcal{F}' = F((p_1 + p_2 - 0.5), p_2; p_1 + p_2; 1 - \frac{c_1}{c_2})$, and F is the hypergeometric function.

If any estimated p value falls below 0.25, it is replaced by $0.25+\epsilon$ so that the parametric L^2-norm can be computed in close form. This norm can be extended in image space to compare two infrared images $\mathbf{I}_1$ and $\mathbf{I}_2$ with parameter values given $(p_1^{(j)}, c_1^{(j)})$ and $(p_2^{(j)}, c_2^{(j)})$ respectively, for $j = 1, 2, \ldots, K$. The image L^2-norm is:

$$d(\mathbf{I}_1, \mathbf{I}_2) = \sqrt{\left(\sum_{j=1}^{K} d(p_1^{(j)}, c_1^{(j)}, p_2^{(j)}, c_2^{(j)})^2\right)}. \quad (6)$$

2.3. Pruning of Hypothesis Space

We follow a method for pruning the hypothesis space based on the image L^2-norm of Eq. (6). The method was originally proposed by Srivastava *et al.* [1, 18]. Specifically, given a test image $\mathbf{I}_t$, a new probability mass function is defined on each image α in the database A as follows:

$$P'(\alpha \mid \mathbf{I}_t) = \frac{1}{Z}\exp\left(-\min_{s\in S} d(\mathbf{I}_t, \mathbf{I}_{\alpha,s})^2/D\right), \quad (7)$$

where

$$Z = \sum_{\alpha'} \exp\left(-\min_{s\in S} d(\mathbf{I}_t, \mathbf{I}_{\alpha,s})^2/D\right).$$

Here, α' represents all images in the database except α, D controls the confidence of our probability, and the Bessel parameters $(p_{\alpha,s}^{(j)}, c_{\alpha,s}^{(j)})$ for each image α in the database rendered at pose s can be computed off-line. Pose, here, refers to a combination of scale σ and orientation θ. All images with probability $P'(\alpha \mid \mathbf{I})$ greater than a threshold ϵ_1 are short-listed as best matches.

2.4. Bayesian Classifier

The pruned hypothesis space produces a small set of highly likely candidates, but not a unique match. We take the process a step further from what was proposed in [1, 18] by applying Bayesian classification on the short list to find the exact match. The Bayesian classifier looks for the subject with the highest posterior probability $P(\alpha \mid \mathbf{I})$, which is calculated as the product of the prior probability density $P(\alpha)$ and the likelihood $P(\mathbf{I} \mid \alpha)$:

$$P(\alpha \mid \mathbf{I}) = \frac{\mathbf{P}(\mathbf{I} \mid \alpha)\mathbf{P}(\alpha)}{\mathbf{P}(\mathbf{I})}, \qquad \text{for } \alpha \in \mathbf{A}. \quad (8)$$

We assume that the priors are equiprobale. If the total number of images in the short list is N, then the prior probability for each likely image α is set to be $\frac{1}{N}$. So, the posterior depends exclusively on the likelihood function $P(\mathbf{I_t} \mid \mathbf{s}, \alpha)$, which quantifies the probability that image α at pose s will give rise to the test image $\mathbf{I_t}$. The likelihood function can be calculated by:

$$P(\mathbf{I_t} \mid \mathbf{s}, \alpha) = \frac{\mathbf{1}}{(\mathbf{2\pi\sigma^2})^{\mathbf{d/2}}} \exp\left(\frac{\mathbf{-1}}{\mathbf{2\sigma^2}}||\mathbf{I_t} - \mathbf{I}_{\alpha,\mathbf{s}}||^{\mathbf{2}}\right). \quad (9)$$

Here, σ is the variance of the test image and $||\mathbf{I_t} - \mathbf{I}_{\alpha,\mathbf{s}}||^{\mathbf{2}}$ is the L^2-norm between test image $\mathbf{I_t}$ and target image $\mathbf{I}_\alpha$ at pose s. Our algorithm computes the posterior probabilities for each image in the short list and classifies the image with the maximum value as a match. If the maximum posterior is less than a threshold ϵ_2, then the algorithm classifies the test image as not being in the database.

3. Results and Discussion

We have tested our method on the Equinox facial database [25]. This is the most extensive infrared facial database that is publicly available at the moment. The Equinox database has a good mix of subject images with accessories (e.g., glasses) as well as expressions of happiness, anger, and surprise, which account for pose variation. Figure 4 shows some examples from this database.

We have used a total of 2750 mid-wave infrared images, which correspond to 50 different subjects. Specifically, we have used 45 subjects at 5 different poses each, as training data. We have also used 50 subjects with 50 images per subject for testing. We have observed that the pruned subset is smaller when the Bessel model is applied on segmented images. Figure 5 depicts the increase we realize in pruning performance when compared to that of [18]. As depicted

Figure 4: Sample images from the Equinox database.

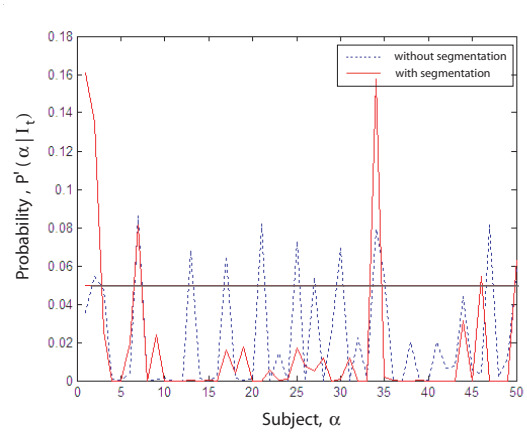

Figure 5: Plot of $P'(\alpha \mid \mathbf{I_t})$ when the Bessel parameters are computed on segmented versus non-segmented images, with subject #7 as the test image. Database subjects are short-listed as the most promising matches if their likelihood is higher than a threshold value (straight line)

in Figure 5, 11 out of 50 images are short-listed as best matches when Bessel models are applied on non-segmented images and subject #7 is used for testing. In contrast, only 5 out of 50 images are short-listed as best matches for the same test image when we use adaptive fuzzy connectedness segmentation. Similar results are produced by all the other subjects in the database.

We have compared the identification performance of our approach with and without segmentation as well as with the eigenfaces method (an earlier appearance-based approach [14]). Figure 6 shows the Precision/Recall graphs of all three methods. Figure 7 shows the receiver operating characteristic (ROC) curve for the same methods. We have also varied the number of test images to check the performance in different conditions.Table 1 provides performance results of the three approaches on the Equinox database at different training/test ratio conditions. In all cases, our approach with segmentation outperforms the other two. It is interesting to point out that the background in the Equinox database is typically uniform and simple. Therefore, it is remarkable that segmentation provides such a boost in identification and pruning performance even in the case of mugshot type images.

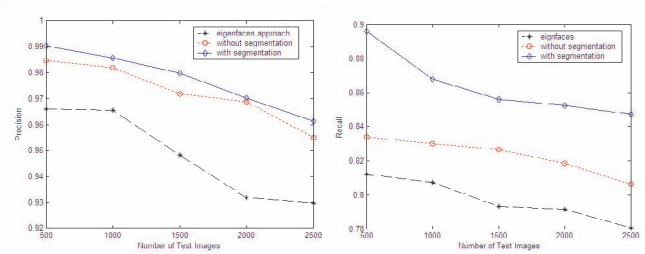

(a) (b)

Figure 6: (a) Precision and (b) Recall graphs of the following approaches: eigenfaces, our method without segmentation, and our method with segmentation.

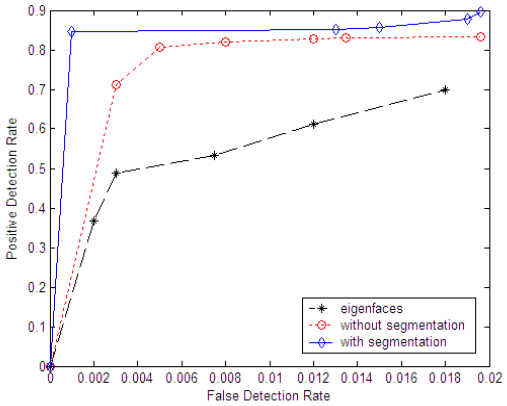

Figure 7: ROC curve of the following approaches: eigenfaces, our method without segmentation, and our method with segmentation.

4. Conclusion

We presented a face recognition method in the infrared spectrum. The choice of infrared makes the system less dependent on external light sources and more robust with respect to incident angle and light variation. The background is removed using adaptive fuzzy connectedness segmentation enhanced by automatic selection of multiple seeds. Features are computed by decomposing the segmented images into their spectral components and modeling them through Bessel forms. The parameters of the Bessel forms constitute the feature vectors, which are used for hypothesis

Test/Training ratio	Eigenfaces	Our method on non-segmented images	Our method on segmented images
2:1	81.21%	83.4%	89.6%
4:1	80.72%	83.01%	86.8%
6:1	79.32%	82.66%	85.6%
8:1	78.68%	81.85%	85.25%
10:1	76.72%	80.60%	84.72%

Table 1: Performance of the eigenfaces, Bessel forms without segmentation, and Bessel forms with segmentation approaches at varying test/training ratios.

pruning. A Bayesian classifier determines a unique solution out of the pruned subset. Our method compares favorably to older approaches such as eigenfaces. Experimental results also show that our method performs better with segmentation rather than without. Finally, our method involves a two-stage classification scheme that produces a unique solution and not a short list of candidates. We are currently working on establishing our own thermal facial database and testing our method further. In contrast to the Equinox database, our database will be temperature calibrated and will include dynamic environmental conditions (e.g., changing environmental temperature and air-flow).

Acknowledgements

This research was supported by NSF grant #0313880 on Information Assurance.

References

[1] Srivastava, A., Liu, X., Thomasson, B., Hesher, C.: Spectral probability models for ir images with applications to IR face recognition. In: Proceedings of IEEE Workshop on Computer Vision Beyond the Visible Spectrum: Methods and Applications, Kauai, Hawaii, USA (2001)

[2] Zhao, W., Chellappa, R., Phillips, P.J., Rosenfeld, A.: Face recognition: A literature survey. ACM Computing Surveys (CSUR) **35** (2003) 399–458

[3] Prokoski, F., Riedel, R.: 9 Infrared Identification of Faces and Body Parts. In: BIOMETRICS: Personal Identification in Networked Society. Kluwer Academic Publishers (1998)

[4] Prokoski, F.: History, current status, and future of infrared identification. In: Proceedings of IEEE Workshop on Computer Vision Beyond the Visible Spectrum: Methods and Applications, Hilton Head Island, South Carolina, USA (2000) 5–14

[5] Socolinsky, D., Wolff, L., Neuheisel, J., Eveland, C.: Illumination invariant face recognition using thermal infrared imagery. In: Proceedings of the IEEE Computer Society Conference on Computer Vision and Pattern Recognition(CVPR 2001). Volume 1., Kauai, Hawaii, United States (2001) 527–534

[6] Pavlidis, I., Symosek, P.: The imaging issue in an automatic face/disguise detection system. In: Proceedings of IEEE Workshop on Computer Vision Beyond the Visible Spectrum: Methods and Applications, Hilton Head Island, South Carolina, USA (2000) 15–24

[7] Wilder, J., Phillips, P., Jiang, C., Wiener, S.: Comparison of visible and infrared imagery for face recognition. In: Proceedings of the Second International Conference on Automatic Face and Gesture Recognition, Killington, Vermont (1996) 182–187

[8] Socolinsky, D., Selinger, A.: A comparative analysis of face recognition performance with visible and thermal infrared imagery. In: Proceedings of 16th International Conference on Pattern Recognition. Volume 4., Quebec, Canada (2002) 217–222

[9] Chen, X., Flynn, P., Bowyer, K.: Pca-based face recognition in infrared imagery: Baseline and comparative studies. In: Proceedings of the IEEE International Workshop on Analysis and Modeling of Faces and Gestures, Nice, France (2003) 127–134

[10] Turk, M., Pentland, A.: Eigenfaces for recognition. J. Cognitive Neuroscience **3** (1991) 71–86

[11] Belhumeur, P., P.Hespanha, J., Kriegman, D.: Eigenfaces vs. fisherfaces: recognition using class specific linear projection. IEEE Transactions on Pattern Analysis and Machine Intelligence **19** (1997) 711–720

[12] Bartlett, M., Movellan, J., Sejnowski, T.: Face recognition by independent component analysis. IEEE Transactions on Neural Networks **13** (2002) 1450–1464

[13] Lu, J., Plataniotis, K., Venetsanopoulos, A.: Face recognition using LDA-based algorithms. IEEE Transactions on Neural Networks **14** (2003) 195–200

[14] Cutler, R.: Face recognition using infrared images and eigenfaces. cs.umd.edu/rgc/face/face.htm (1996)

[15] Yoshitomi, Y., Miyawaki, N., Tomita, S., Kimura, S.: Facial expression recognition using thermal image processing and neural network. In: Proceedings of 6th IEEE International Workshop on Robot and Human Communication. (1997) 380–385

[16] Phillips, P.: Matching pursuit filters applied to face identification. IEEE Transactions on Image Processing **7** (1998) 1150–1164

[17] Campadelli, P., Savazzi, R.L.C.: A feature-based face recognition system. In: Proceedings of 12th International Conference on Image Analysis and Processing, Mantova, Italy (2003) 68–73

[18] Srivastava, A., Liu, X.: Statistical hypothesis pruning for recognizing faces from infrared images. Journal of Image and Vision Computing **21** (2003) 651–661

[19] Pednekar, A., Kakadiaris, I., Kurkure, U.: Adaptive fuzzy connectedness-based medical image segmentation. In: Proceedings of the Indian Conference on Computer Vision, Graphics, and Image Processing, Ahmedabad, India (2002) 457–462

[20] Srivastava, A., Miller, M.I., Grenander, U.: Bayesian automated target recognition. In: Handbook of Image and Video Processing. Academic Press (2000) 869–881

[21] Udupa, J., Samarasekera, S.: Fuzzy connectedness and object definition: Theory, algorithms, and applications in image segmentation. Graphical Models and Image Processing **58** (1996) 246261

[22] Udupa, J., Samarasekera, S.: Fuzzy connectedness and object definition. In: SPIE Proceedings Medical Imaging. Volume 2431. (1995) 2–10

[23] Mittal, N., Mital, V., Luk, C.: Features for texture segmentation using Gabor filters. In: Seventh International Conference on Image Processing And Its Applications. Volume 1., Manchester, UK (1999) 353–357

[24] Grigorescu, S., Petkov, N., Kruizinga, P.: Comparison of texture features based on gabor filters. IEEE Transactions on Image Processing **11** (2002) 1057–7149

[25] Equinox: Face database. equinoxsensors.com/products/HID.html (2004)